Simple Feedforward Carrier Phase Estimation for Optical FBMC/OQAM Systems

Trung-Hien Nguyen, *Member*, *IEEE*, Jérome Louveaux, *Member*, *IEEE*, Simon-Pierre Gorza and François Horlin, *Member, IEEE*

***Abstract*—Filter-bank multi-carrier based on offset quadrature amplitude modulation (FBMC/OQAM) has recently been proposed to improve the spectral efficiency of optical fiber communication systems. Unfortunately, it is prone to the laser phase noise (PN) that results in significant inter-subcarrier interference due to the loss of OQAM orthogonality. Based on the analysis of the OQAM constellation obtained at the output of the analysis filter bank, we propose a modified blind phase search (M-BPS) algorithm working based on the observation of all subcarriers simultaneously. It efficiently compensates for the PN and incurs a low number of multiplications. The proposed method is analytically derived and numerically validated with 4–, 16– and 64–OQAM modulations. The impact of the number of subcarriers used per optical channel is also investigated. The results show that up to 256 subcarriers can be utilized with negligible performance degradation. Moreover, the method provides a tolerated linewidth and symbol duration product of $1.4\cdot10^{-4}$, $2.5\cdot10^{-5}$ and $6.2\cdot10^{-6}$ for respective 4–, 16– and 64–OQAM modulations to limit the SNR penalty to 1 dB at a BER of 10^{-3}.**

***Index Terms*—Filter-bank multicarrier, offset QAM, coherent detection, carrier phase estimation.**

I. Introduction

FILTER-BANK multi-carrier based on offset quadrature amplitude modulation (FBMC/OQAM), an alternative to orthogonal frequency-division multiplexing (OFDM), has recently received much attention in optical fiber communication systems [1-6]. Compared to OFDM, FBMC uses shaping filters featuring a better time/frequency localization, making FBMC systems more robust to time-varying effects. Moreover, the orthogonality between adjacent overlapping channels is ensured by using the OQAM modulation [5].

Up to now, most proposed applications of FBMC/OQAM to optical fibers communications only consider a small number of OQAM subcarriers (if not only one) per optical carrier [1–5]. In such systems, it is not necessary to insert a frequency gap between optical carriers to prevent inter-carrier interference thanks to the OQAM orthogonality, resulting in a better spectral efficiency (SE). Furthermore, the digital signal processing (DSP) implemented at the receiver side to compensate for the channel impairments is usually applied per subcarrier in order to take the advantage of the multi-carrier modulation for parallel processing. When the number of subcarriers is small, an equalizer taking the form of a filter of finite impulse response should be used to compensate for the inter-symbol interference caused by the channel memory. Additionally, the laser phase noise (PN) causes interference between the FBMC/OQAM subcarriers along with the constellation rotation [1]. Consequently, the conventional carrier phase estimation (CPE) used in QAM systems cannot be directly applied. Several solutions for PN compensation have been proposed so far. An innovative phase tracking algorithm is designed in [2] to minimize the error at the output of the equalizer. A modified feedforward blind phase search algorithm (M-BPS) is introduced in [1] and its reduced complexity versions are presented in [3-4]. While the first algorithm requires an additional feedback loop, the second algorithm suffers from a high computational effort.

In the multi-subcarrier FBMC/OQAM systems [6], increasing the number of subcarriers allows the low complexity one-tap equalizer to efficiently compensate for the channel impairments like the chromatic dispersion (CD). However, with the increase of subcarrier number, the PN variation over the time is no longer negligible compared to the symbol duration. In this case, methods in [1–4] are no longer suitable. In [6], a pilot-based method for PN compensation has been utilized, however, suffering from the reduced SE due to the pilot addition.

In this paper, a simple M-BPS is proposed to compensate for the PN in the frequency domain. The data on all subcarriers at the output of the analysis filter bank (AFB) are used to estimate the PN at each symbol time. This distinguishes the proposed algorithm to the per-subcarrier PN compensation methods. We derive the algorithm analytically, showing its optimality in the maximum likelihood (ML) sense. Compared to other M-BPS methods, the distance calculation in the complex plane in M-BPS is simplified by considering only the distance in the real plane. This allows a significant reduction of the number of multiplications, providing less computational efforts. The proposed methods are numerically validated in FBMC systems with 4–, 16– and 64–OQAM

This work is supported by the Belgian Fonds National de la Recherche Scientifique (FNRS) under Grant PDR T.1039.15.

T.-H. Nguyen, S.-P. Gorza and F. Horlin are with OPERA department, Université libre de Bruxelles, 1050 Brussels, Belgium (e-mail: trung-hien.nguyen@ulb.ac.be; simon-pierre.gorza@ulb.ac.be; francois.horlin@ulb.ac.be).

J. Louveaux is with ICTEAM institute, Université catholique de Louvain, 1348 Louvain-la-Neuve, Belgium (e-mail: jerome.louveaux@uclouvain.be).

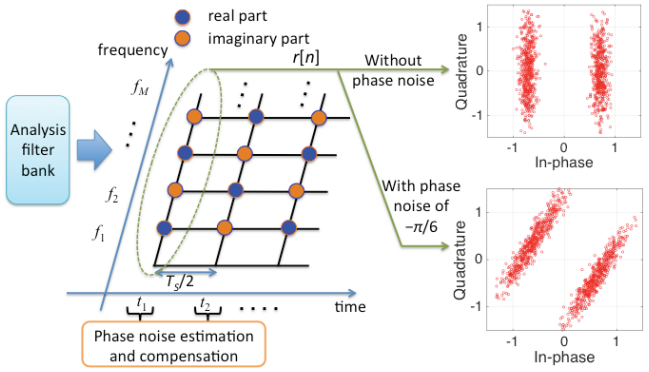

Fig. 1. Time-frequency presentation of OQAM signals after the analysis filter bank and the 4OQAM constellation examples at the time instance t_1 without phase noise (upper) and with phase noise of $-\pi/6$ (lower).

signals. Finally, the effectiveness of the simplified M-BPS is also investigated in terms of the optimum number of used subcarriers and the laser linewidth tolerance.

II. Phase Noise Influence on FBMC/OQAM

In order to focus on the laser phase noise effect, only one polarization is considered. However the results can easily be extended to dual-polarization systems. Ideal time/frequency synchronization and perfect compensation of the chromatic dispersion are assumed. The random binary sequences are mapped on QAM complex symbols of duration T. The real and imaginary parts of generated symbols are then passed to the OQAM preprocessing stage, where they are transmitted with a delay of $T/2$. Moreover, a $\pi/2$ phase difference is introduced between adjacent subcarriers to ensure their orthogonality. The efficient inverse fast-Fourier transform/ fast-Fourier transform (IFFT/FFT) based implementation is applied at the synthesis filter bank (SFB) and the AFB [7]. Note that, the sample rate at the output of SFB is $1/T_S = M/T$, where M is the number of subcarriers. The square-root raised cosine filter with roll-off factor of 1 is used as the prototype filter. It is noted that other prototype filters can be applied as long as they satisfy the Nyquist criterion [8]. In our cases, the roll-off factor of 1 is chosen to achieve the low complexity time domain implementation of the filter.

At the transmitter, all the subcarriers after the SFB are summed up together. This signal is then corrupted by the additive Gaussian white noise (AWGN) and loaded with the laser PN. The PN is modeled as a discrete random time walk $\varphi_m = \varphi_{m-1}+\Theta_m$, where Θ_m denotes the PN variation on the sample m. It is modeled as a zero-mean Gaussian random variable of variance $2\pi\cdot\Delta\nu\cdot T_S$. The parameter $\Delta\nu$ denotes the laser linewidth. At the receiver, the inverse processes are carried out to recover the data. Fig. 1 illustrates the outputs of AFB in the time/frequency diagram. Considering the 4–OQAM samples of all subcarriers at the time instant t_1, the constellation points are located at $\pm 1/\sqrt{2}$ on the real axis and dispersed vertically along the imaginary axis in the absence of PN. In this case, the received OQAM symbol can be recovered without interference by taking the real part of the received complex signals. However, in the presence of PN, the constellation is rotated resulting in the interference at the symbols of interest after the OQAM post-processing stage (see in Fig.1 for $\varphi_n = -\pi/6$). The PN compensation is therefore compulsory in order to recover the transmitted symbols without interference. Based on the observation of the specific OQAM constellations with and without phase noise, we will extend the BPS algorithm to effectively compensate for the PN in FBMC/OQAM systems.

III. Simple Feedforward Modified BPS Algorithm

Considering FBMC/OQAM systems with a sufficiently slow-varying φ_n with regards to the n-th FBMC symbol duration, the AFB output after the one-tap channel equalizer can be written for subcarrier k and instant n as [7]

$$r_{k,n} = \left(I_{k,n} + j\cdot u_{k,n}\right)e^{j\varphi_n} + \omega_{k,n}, \tag{1}$$

where $I_{k,n}$ is the real or imaginary part of the QAM symbols and $u_{k,n}$ is the interference coming from the neighboring symbols on the carrier of interest and on the adjacent subcarriers. The interference term, $j\cdot u_{k,n}$, is purely imaginary in the absence of PN. In order to obtain a simple estimator, we make the simplifying assumption that $u_{k,n}$ is independent of the transmitted data, with mean equal to zero and variance denoted by σ_u^2. The term $\omega_{k,n}$ is the zero mean AWGN of variance σ_ω^2 for both real and imaginary parts. When there is no PN ($\varphi_n = 0$), the symbols are generally estimated by taking the real part of $r_{k,n}$ removing therefore completely the interference.

We denote by X^R (resp. X^I) the real (resp. imaginary) part of the variable X, and $(\cdot)^T$ is the transpose operator. Considering all subcarriers ($k = 1,\ldots, M$) at instant n, (1) can be reformulated as

$$\underline{r}_n = \underline{I}_n \otimes \underline{\varphi}_n + \underline{v}_n, \tag{2}$$

where the received vector is $\underline{r}_n = \left(r_{1,n}^R \;\; r_{1,n}^I \;\; r_{2,n}^R \;\; r_{2,n}^I \ldots r_{M,n}^R \;\; r_{M,n}^I\right)^T$, the symbol vector is $\underline{I}_n = \left(I_{1,n} \;\; I_{2,n} \ldots I_{M,n}\right)^T$, the phase noise vector is $\underline{\varphi}_n = \left(\cos\varphi_n \;\; \sin\varphi_n\right)^T$, and the noise vector is $\underline{v}_n = \left(v_{1,n}^R \;\; v_{1,n}^I \;\; v_{2,n}^R \;\; v_{2,n}^I \ldots v_{M,n}^R \;\; v_{M,n}^I\right)^T$. The elements of the noise vector, defined as $v_{k,n}^R = -u_{k,n}\sin\varphi_n + \omega_{k,n}^R$ and $v_{k,n}^I = u_{k,n}\cos\varphi_n + \omega_{k,n}^I$, both include the AWGN and the interference. The operator $\otimes$ is the Kronecker product.

To simplify the notation, the index n is omitted in the following derivation. The likelihood function of M subcarriers samples $\underline{r}$, knowing the transmitted OQAM signals $\underline{I}$ and phase noise φ_n, can be written as

$$f\left(\underline{r}\middle|\underline{I},\varphi_n\right) = \frac{1}{\sqrt{(2\pi)^{2M}\det\left(\underline{\underline{R}}_v(\varphi_n)\right)}} \exp\left(-\frac{1}{2}\left(\underline{r}-\underline{I}\otimes\varphi_n\right)^T\left(\underline{\underline{R}}_v(\varphi_n)\right)^{-1}\left(\underline{r}-\underline{I}\otimes\varphi_n\right)\right), \tag{3}$$

in which the term $\det\left(\underline{\underline{R}}_v(\varphi_n)\right)$ is the determinant of the covariance matrix $\underline{\underline{R}}_v(\varphi_n) = E\left[\underline{v}\cdot\underline{v}^H\right]$. It is a $2M\times 2M$ block-

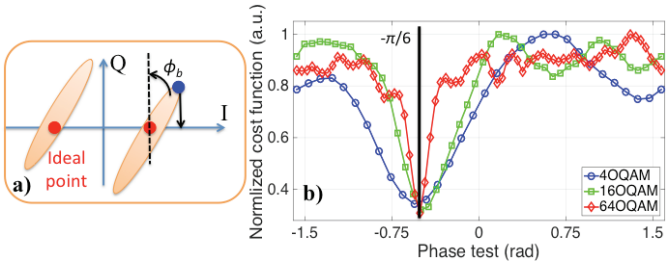

Fig. 2. a) Illustration of the 4-OQAM constellation rotation in order to find the phase noise value based on the minimization of distance between the projection on the real axis and the ideal points. b) Normalized cost functions of 4-, 16- and 64-OQAM signals for a phase noise value of $-\pi/6$.

diagonal matrix that contains M 2×2 matrices R_{v_n} on its diagonal equal to

$$R_{v_n} = \begin{pmatrix} \frac{\sigma_u^2}{2}(1-\cos 2\varphi_n)+\sigma_\omega^2 & -\frac{\sigma_u^2}{2}\sin 2\varphi_n \\ -\frac{\sigma_u^2}{2}\sin 2\varphi_n & \frac{\sigma_u^2}{2}(1+\cos 2\varphi_n)+\sigma_\omega^2 \end{pmatrix}, \quad (4)$$

where $E[\cdot]$and $(\cdot)^H$ are the expectation and Hermitian transpose, respectively. After some mathematical manipulation, the logarithmic likelihood function is expressed as

$$\log f\left(\underline{r}|\underline{I},\varphi_n\right) = C + \frac{1}{2}\sum_{k=1}^{M}\left(\frac{|I_k|^2}{\sigma_u^2} - \frac{|r_k|^2}{\sigma_u^2+\sigma_\omega^2}\right) - \frac{1}{2}\sum_{k=1}^{M}\left(\frac{\sigma_u}{\sigma_\omega\sqrt{\sigma_u^2+\sigma_\omega^2}}\mathrm{Re}\left(r_k\cdot e^{-j\varphi_n}\right) - \frac{I_k\sqrt{\sigma_u^2+\sigma_\omega^2}}{\sigma_u\sigma_\omega}\right)^2, \quad (5)$$

in which $C = -\log\left(2\pi\sigma_\omega\sqrt{M\left(\sigma_u^2+\sigma_\omega^2\right)}\right)$. The maximum likelihood (ML) estimate consists in maximizing (5). The maximum is given by

$$\max \log f\left(\underline{r}|\underline{I},\varphi_n\right) = C + \frac{1}{2}\sum_{k=1}^{M}\left(\frac{|I_k|^2}{\sigma_u^2} - \frac{|r_k|^2}{\sigma_u^2+\sigma_\omega^2}\right), \quad (6)$$

This maximum value can be obtained when the following condition is satisfied

$$\sum_{k=1}^{M}\left(\mathrm{Re}\left(r_k\cdot e^{-j\varphi_n}\right) - \left(1+\sigma_\omega^2/\sigma_u^2\right)\cdot I_k\right) = 0. \quad (7)$$

Inspection of (7) reveals that the ML estimator is a 2–dimensional estimation problem. Each received sample is rotated in the complex plane by the test phase and projected on the real axis where it is coherently compared to the weighted estimated I_k. The weight depends on the ratio between variances of noise (σ_ω^2) and of interference (σ_u^2). In practice, the values of variances are however not known. In the moderate and high signal-to-noise ratio (SNR) regions, $\sigma_\omega^2 \ll \sigma_u^2$ is usually a valid assumption enabling an approximate ML estimator that is independent of the noise and interference variances.

To implement (7), we therefore propose to test progressively all values of the phase, ϕ_b, on a pre-defined grid, and to select the one that minimizes the sum of distances between the projections on the real axis of the received samples after test phase compensation and their hard decision versions. The hard decision is made by comparing the projection of the received sample to the ideal points of the pulse-amplitude modulation (PAM) and selecting the closet one. Fig. 2(a) illustrates the phase rotation applied in case of a 4–OQAM constellation. The estimated phase rotation can be expressed by

$$\hat{\phi}_b = \arg\min_{\phi_b}\sum_{k=1}^{M}\left|\mathrm{Re}\left(\hat{r}_{k,n,b}\right) - DD\left(\mathrm{Re}\left(\hat{r}_{k,n,b}\right)\right)\right|, \quad (8)$$

in which DD is the direct decision operator and the rotated version of $r_{k,n}$ is $\hat{r}_{k,n,b} = r_{k,n}\cdot\exp\left(-j\cdot\phi_b\right)$. The grid is defined as $\phi_b = (b/B)\cdot\pi - \pi/2$, where $b = 1, 2, \ldots, B$ and B is the total number of phase tests. The impact of the additive noise is reduced by averaging the cost function over M subcarriers. The rotated samples version corresponding to each phase test is then sent to a switch that selects the best phase rotation to alleviate the phase noise impact.

In terms of complexity, the distance calculations in the simplified M-BPS algorithm are carried out in real plane by taking only the real part of the rotated sample version. Compared to the traditional M-BPS [1], where each distance calculation requires computation of the square norm of a complex number, the simplified distance calculation no longer requires any multiplications. Fig. 2(b) shows the examples of cost functions for the simplified M-BPS method at the phase noise value of $-\pi/6$, for different OQAM signals. It can be observed that the cost functions exhibit the same minimum value at about $-\pi/6$, i.e. the value of the phase noise φ_n. The effectiveness of the proposed algorithm has been evaluated with a random time walk laser phase noise model.

IV. Results and Discussion

The performance of the 30 Gbaud 4–, 16– and 64–OQAM systems is assessed in this section. The SNR is fixed to a value 1 dB larger than the SNR needed to achieve a BER equal to 10^{-3}. Consequently, SNRs of 7.8 dB, 11.7 dB and 15.8 dB are employed for 4–, 16– and 64–OQAM signals, respectively. Unless stated otherwise, the number of subcarriers is chosen equal to 256 for all modulation orders. The normalized linewidths (i.e. the product of the laser linewidth by the symbol duration), $\Delta\nu\cdot T_S$, are set to $1.5\cdot10^{-5}$, $5\cdot10^{-6}$ and $2.5\cdot10^{-6}$ for 4–, 16– and 64–OQAM signals, respectively.

The optimum number of phase tests, defined as the smallest number of phase tests necessary to reach the target BER, is firstly studied. It is an important metric that quantifies the trade-off between the system performance and the implementation complexity. Fig. 3(a) shows the evaluated BER as a function of the number of phase tests, B for 4–, 16– and 64–OQAM, respectively. It can be seen that the BER first rapidly improves with the number of phase tests and then remains constant. The optimum number of phase tests for 4–,

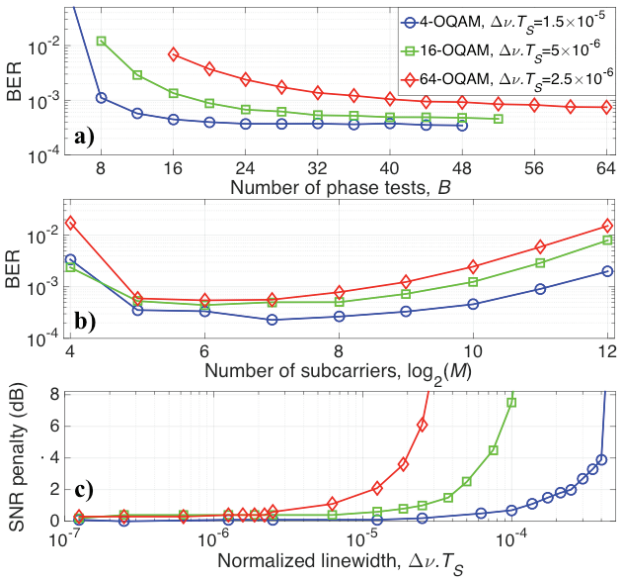

Fig. 3. a) BER versus the number of phase test angles, B. b) BER as a function of the number of subcarriers, M. c) SNR penalty versus normalized linewidths, $\Delta\nu{\cdot}T_S$.

16– and 64–OQAM signals are 16, 32 and 56, respectively. Hereafter, the number of phase tests is fixed to their optimal values.

The BER for a varying number of subcarriers, M, is investigated in Fig. 3(b) for different modulation orders. It can be observed that the BER rapidly decreases when M increases from 16 to 32. It is due to the better averaging of the AWGN when the sample set becomes larger. However, as the subcarriers number grows the FBMC symbol duration becomes larger. As a consequence, the assumption of constant-PN over the symbol duration does not hold for too large M, resulting in an increase of the BER as shown in Fig. 3(b). The maximum number of subcarriers for 4–, 16– and 64–OQAM are 2048, 512 and 256, respectively to achieve a 1 dB SNR penalty at a 10^{-3} BER. The compromise between the AWGN and the laser PN can affect the choice of the optimum number of subcarriers. It should be reminded that the number of subcarriers might need to maximize enabling to efficiently compensate for the CD in optical FBMC systems. A value of $M = 256$ is hence a good trade-off to ensure negligible performance degradation regarding the PN considered. The SNR penalties at a BER = 10^{-3} for various normalized linewidths are further investigated in Fig. 3(c) for different modulation orders. It can be seen that the maximum tolerated normalized linewidths to limit the SNR penalty below 1 dB are $1.4{\cdot}10^{-4}$, $2.5{\cdot}10^{-5}$ and $6.2{\cdot}10^{-6}$ for 4–, 16– and 64–OQAM respectively. Considering a 30 Gbaud FBMC systems, the tolerated laser linewidths are thus 4.2 MHz, 750 kHz and 190 kHz for 4–, 16– and 64–OQAM, respectively. This confirms the effectiveness of the proposed as these linewidths are compatible with commercial lasers.

As discussed in [6], the accumulated CD can effectively be compensated with a simple one-tap equalizer per subcarrier thanks to the nearly constant channel response on a subcarrier. Selecting the parameters according to [6], we further evaluate the BER after 100 km, 50 km and 25 km standard single mode

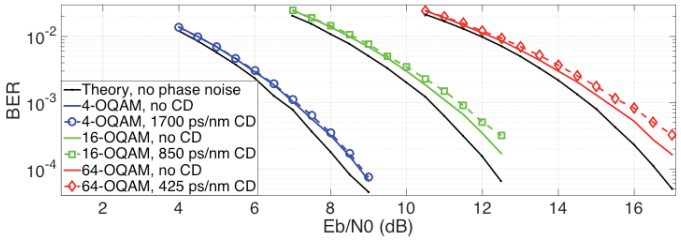

Fig. 4. Evolutions of BER of 4-, 16- and 64-OQAM as the function of bit power over noise power, Eb/N0, with and without CD.

fiber (SSMF) transmission for 4–, 16– and 64–OQAM, respectively (CD equals to 17 ps/nm/km for SSMF). Afterward, the proposed PN compensation is applied. Fig. 4 illustrates the BER as a function of the SNR. In the presence of PN only, a SNR penalty smaller than 0.4 dB at a 10^{-3} BER remains at the output of the M-BPS algorithm. In the presence of both the PN and CD, an additional SNR penalty smaller than 0.3 dB at a 10^{-3} BER is observed for 16– and 64–OQAM because there also exists a residual CD at the output of the one-tap equalizer that impacts both the performance of the subsequent M-BPS algorithm and symbol detection [6]. Not surprisingly, the figure shows that the impact of channel impairments increases with the modulation order. It should be noted that the transmission distance could be further extended up to M times by applying the CD compensation technique in [6].

V. Conclusion

We have proposed a simple feedforward carrier phase estimation method for optical FBMC/OQAM systems that can reduce the computational effort compared to the traditional M-BPS method. The proposed method has been analytically derived and validated with 4–, 16– and 64–OQAM signals. It has been shown that the algorithm can work with 256 subcarriers without performance degradation and the tolerated linewidth is in the range of commercial lasers.

References

[1] H. Tang, M. Xiang, S. Fu, M. Tang, P. Shum, and D. Liu, "Feed-forward carrier phase recovery for offset-QAM Nyquist WDM transmission," *Opt. Express*, vol. 23, no. 5, pp. 6215-6227, Mar. 2015.

[2] J. Fickers, A. Ghazisaeidi, M. Salsi, G. Charlet, P. Emplit, and F. Horlin, "Multicarrier offset-QAM for long-haul coherent optical communications," *J. Lightw. Technol.*, vol. 32, no. 24, pp. 4069-4076, Dec. 2014.

[3] T.-H. Nguyen, S.-P. Gorza, J. Louveaux, and F. Horlin, "Low-complexity blind phase search for filter bank multicarrier offset-QAM optical fiber systems," in *Proc. SPPcom 2016*, Vancouver, Canada, Jul. 2016, p. SpW2G.2.

[4] J. Lu, S. Fu, H. Tang, M. Xiang, M. Tang, D. Liu, "Vertical blind phase search for low-complexity carrier phase recovery of offset-QAM Nyquist WDM transmission," Opt. Commun., vol. 382, pp. 212-218, Jan. 2017.

[5] F. Horlin, J. Fickers, P. Emplit, A. Bourdoux, and J. Louveaux, "Dual-polarization OFDM-OQAM for communications over optical fibers with coherent detection," *Opt. Express*, vol. 21, no. 5 pp. 6409-6421, Mar. 2013.

[6] J. Zhao and P. D. Townsend, "Dispersion tolerance enhancement using an improved offset-QAM OFDM scheme," *Opt. Express*, vol. 23, no. 13, pp. 17638-17652, Jun. 2015.

[7] P. Siohan, C. Siclet, and N. Lacaille, "Analysis and design of OFDM/OQAM systems based on filterbank theory," *IEEE Trans. Signal Processing*, vol. 50, no. 5, pp. 1170-1183, May 2002.

[8] M. Bellanger *et al.*, "FBMC physical layer: a primer," PHYDYAS project, 2010. Available: http://www.ict-phydyas.org.